Pergamon

Electrochimica Acta, Vol. 40, No. 18, pp. 2979–2984, 1995

0013–4686/95 $9.50 + 0.00

0013–4686(95)00231–6

EFFECT OF CONCENTRATION POLARIZATION ON THE CURRENT–VOLTAGE CHARACTERISTICS OF ION TRANSFER ACROSS ITIES

KYÖSTI KONTTURI,*† JOSÉ A. MANZANARES and LASSE MURTOMÄKI

Department of Thermodynamics, Faculty of Physics, University of Valencia, E-46100 Burjassot, Spain
* Laboratory of Physical Chemistry and Electrochemistry, Helsinki University of Technology, Kemistintie 1A, FIN-02150 Espoo, Finland

(*Received* 11 *November* 1994; *in revised form* 15 *March* 1995)

Abstract—Current-voltage characteristics of ion transfer across the ITIES was theoretically studied, taking concentration polarization into account through the Nernst-Planck equation in the diffusion boundary layers. In the inner layer transport was modelled using either Butler-Volmer or Nernst-Planck equations. Potential distribution across the ideally polarizable ITIES was calculated from the Poisson-Bolzman equation. The current-voltage curves were of the Butler-Volmer type, but no distinction between the two approaches inside the inner layer could be seen because the permeability of the entire system was determined by the diffusion boundary layers.

Key words: current-voltage characteristics, ITIES, ion transfer, Nernst-Planck equation, concentration polarization.

INTRODUCTION

Current-voltage characteristics of ion transfer (IT) across the interface between two immiscible electrolyte solutions (ITIES) has been subject to several theoretical and experimental studies in the last decade[1]. The models used to describe IT have always been closely related to the models of the interfacial structure. In the earliest papers, the interfacial region was modelled as two diffuse double layers back-to-back[2]. Later treatments proposed the existence of a compact layer[3] or an ion-free layer[4] which acts as an energy barrier for IT. The height of such a barrier has even been estimated to be 14–17 kJ mol^{-1}[5]. Currently the most widely accepted model considers the 'inner layer' as a mixed solvent layer where dielectric properties are changing smoothly from one phase to another[6]. This model has been corroborated by recent molecular dynamics simulations which allow us to estimate the thickness of this transition region as *ca.* 1 nm in the case of water/1,2-dichloroethane interface[7].

The earliest models of IT assumed kinetic control described by Butler-Volmer type expressions and the first measurements yielded values for the standard rate constant k^0 of the order of 10^{-3} cm s^{-1} (*eg*, Ref. [3]). Later values, calculated from convolution sweep voltammetry, were of the order of 10^{-1} cm s^{-1}[8]. Quite recently, the availability of a micro ITIES techniques which further enhances the rate of mass transfer has made it possible to observe reversible transfer of small ions (*ie*, k^0 is at least of the order of 1 cm s^{-1})[9]. Therefore, it seems reasonable not to invoke the assumption of kinetic control of IT. Modelling of IT across the inner layer, if needed at all, does not necessarily require the use of Butler-Volmer type equations. In fact, Kakiuchi has lately shown that current-voltage characteristics of IT can be derived from Nernst–Planck type equations[10], and molecular dynamic simulations has shown that ionic motion across the inner layer is more likely similar to that in the bulk solution[7,11].

Regardless of the use of Butler-Volmer or Nernst-Planck type equations for the description of IT across the inner layer, the surface concentrations, *ie*, the concentrations at the two boundaries of this layer, have to be evaluated. Although the correction for the diffuse double layer (Frumkin correction) has often been made (*eg*, Ref. [12]), concentration polarization has not been systematically studied at the ITIES. Furthermore, the classical treatments of ion transport within electric double layers[13] are not directly applicable to the study of ITIES. In this paper, we use some simple models for the potential distribution across of the ITIES and discuss about the importance of the concentration polarization in IT in terms of the relative permeabilities of the inner layer and the diffusion boundary layers.

FORMULATION OF THE PROBLEM

The system considered here is presented in Fig. 1: An ITIES is created bringing an organic solution 'o' into a contact with an aqueous solution 'w'. The solutions are mutually insoluble and their relative permittivities are ε^o and ε^w, respectively. Across the whole system a potential difference $\Delta_o^w\Phi$ is applied. The base electrolytes of the two solutions are not able to cross the interface, so that an ideally polarizable interface is formed. The potential distribution is

† To whom correspondence should be addressed.

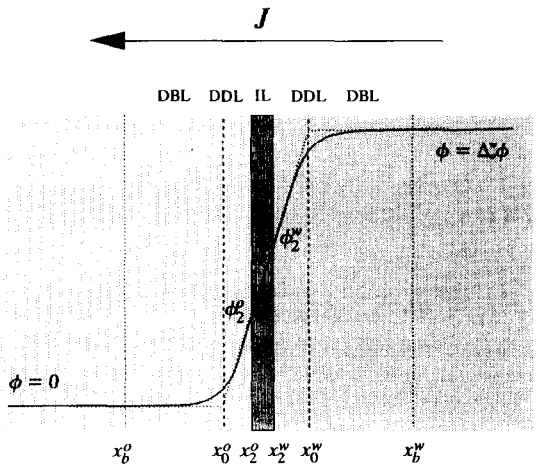

Fig. 1. A schematic view of the ITIES.

determined by the base electrolytes according to the Poisson–Bolzman equation. Thus, the interfacial region consists of an inner layer (IL) flanked by two diffuse double layers (DDL).

A univalent tracer cation is transferred across the interface. Its bulk concentrations are c_b^w and c_b^o, and standard electrochemical potentials $\mu^{0,w}$ and $\mu^{0,o}$, in the appropriate phases. Since concentration polarization is more important when the transferring ion is a tracer ion, the existence of the diffusion boundary layers (DBL) has to be considered (see Fig. 1). The DDLs are then considered to be part of the corresponding DBLs. The other quantities in the different layers are explained the best in Fig. 1.

The ion flux across this composite system (IL + DBLs) can formally be expressed as

$$J = -P(c_b^w e^{\Delta_o^w\phi - \Delta_o^w\phi^0} - c_b^o) \tag{1}$$

where P is the permeability of the system, $\Delta_o^w\phi = \phi_b^w - \phi_b^o$ is the applied potential difference in RT/F units, and $\Delta_o^w\phi^0 = (\mu^{0,w} - \mu^{0,o})/RT$ is the dimensionless standard transfer potential; F, R and T have their usual significance. At steady state the ion flux is continuous and expressions similar to equation (1) can be written for each layer. Thus,

$$J = -P_{DBL}^w(c_b^w e^{\Delta_o^w\phi - \Delta_o^w\phi^0} - c_2^w e^{\phi_2^w - \Delta_o^w\phi^0}) \tag{2}$$

$$J = -P_{IL}(c_2^w e^{\phi_2^w - \Delta_o^w\phi^0} - c_2^o e^{\phi_2^o}) \tag{3}$$

$$J = -P_{DBL}^o(c_2^o e^{\phi_2^o} - c_b^o) \tag{4}$$

Here ϕ_2^w and ϕ_2^o are the potentials at the boundaries of the IL (see Fig. 1). Also, it has been assumed that the standard chemical potential of the tracer changes from $\mu^{0,w}$ to $\mu^{0,o}$ inside the IL.

The permeabilities of the DBLs can easily be obtained from generalized Nernst-Planck equations. The flux of the tracer in the aqueous DBL is given by

$$J = -D^w\left(\frac{dc}{dx} + c\frac{d\phi}{dx} + \frac{c}{RT}\frac{d\mu^o}{dx}\right)$$

$$= -D^w\left(\frac{dc}{dx} + c\frac{d(\phi - \phi^o)}{dx}\right) \tag{5}$$

Integrating over the DBL, equation (5) takes the form

$$J\int_{x_2^w}^{x_b^w} e^{\phi - \phi^o}\,dx = -D^w(c_b^w e^{\Delta_o^w\phi - \Delta_o^w\phi^0} - c_2^w e^{\phi_2^w - \Delta_o^w\phi^0}) \tag{6}$$

so that

$$P_{DBL}^w = \frac{D^w}{\int_{x_2^w}^{x_b^w} e^{\phi - \phi^o}\,dx} \tag{7}$$

Analogously,

$$P_{DBL}^o = \frac{D^o}{\int_{x_b^o}^{x_2^o} e^{\phi - \phi^o}\,dx} \tag{8}$$

We have mentioned in the Introduction that IT across the IL can be modelled either from Nernst-Planck or Butler-Volmer equations: If the former approach is followed, the permeability P_{IL} is given by

$$P_{IL}^{N-P} = \frac{D^{IL}}{\int_{x_2^o}^{x_2^w} e^{\phi - \phi^o}\,dx} \tag{9}$$

If the flux is described by the Butler-Volmer type equation

$$J = -k^0[c_2^w e^{\alpha(\phi_2^w - \phi_2^o - \Delta_o^w\phi^0)} - c_2^o e^{(\alpha-1)(\phi_2^w - \phi_2^o - \Delta_o^w\phi^0)}] \tag{10}$$

the P_{IL} is given by

$$P_{IL}^{B-V} = k^0 e^{(\alpha-1)(\phi_2^w - \Delta_o^w\phi^0) - \alpha\phi_2^o} \tag{11}$$

Finally, the permeability of the composite system can be obtained from equations (1)–(4) as

$$\frac{1}{P} = \frac{1}{P_{DBL}^w} + \frac{1}{P_{IL}} + \frac{1}{P_{DBL}^o} \tag{12}$$

In the next sections, these permeabilities will be calculated using different potential distributions, and the IL effects will be analyzed.

POTENTIAL DISTRIBUTION FROM POISSON-BOLZMAN EQUATION

Poisson-Bolzman equation takes the following form in the different parts of the system under study:

$$\frac{d^2\phi}{dx^2} = 2\kappa^w \sinh(\phi - \Delta_o^w\phi) \qquad x > x_2^w \tag{13a}$$

$$\frac{d}{dx}\left(\varepsilon\frac{d\phi}{dx}\right) \approx 0 \qquad x_2^o < x < x_2^w \tag{13b}$$

$$\frac{d^2\phi}{dx^2} = 2\kappa^o \sinh(\phi) \qquad x < x_2^o \tag{13c}$$

Its solution is

$$\phi = \Delta_o^w\phi - 4\tanh^{-1}$$

$$\times \{\tanh[(\Delta_o^w\phi - \phi_2^w)/4]\exp[\kappa^w(x_2^w - x)]\}$$

$$x > x_2^w \tag{14a}$$

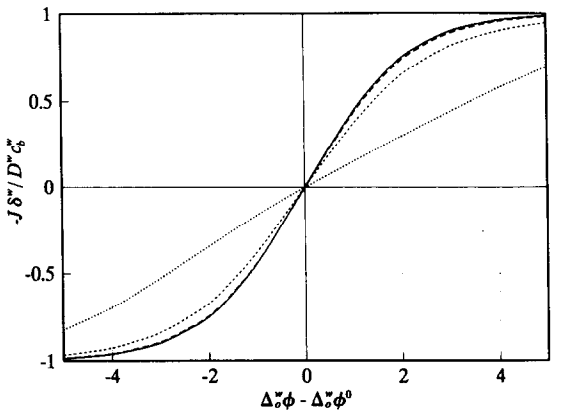

Fig. 2. Current-voltage curves for Poisson-Bolzman potential distribution; Nernst-Planck approach inside the IL with different ratios of D^w/D^{IL} : 0 (No IL, solid); 10^2 (long dashed); 10^3 (dashed); 10^4 (dotted).

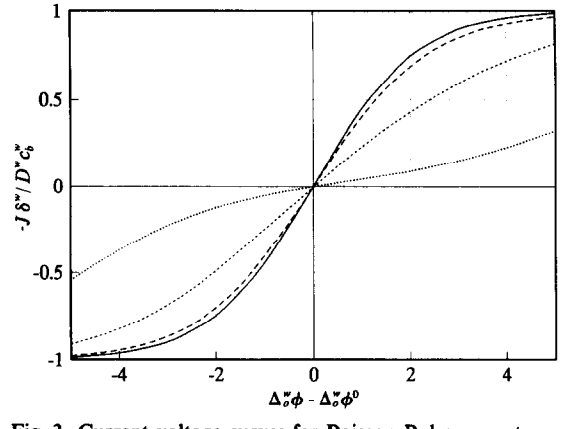

Fig. 3. Current-voltage curves for Poisson-Bolzman potential distribution, Butler-Volmer approach inside the IL with $\alpha = 0.5$ and different values of k^0 (cm s^{-1}): ∞ (reversible, solid); 10^{-1} (long dashed); 10^{-2} (dashed); 10^{-3} (dotted).

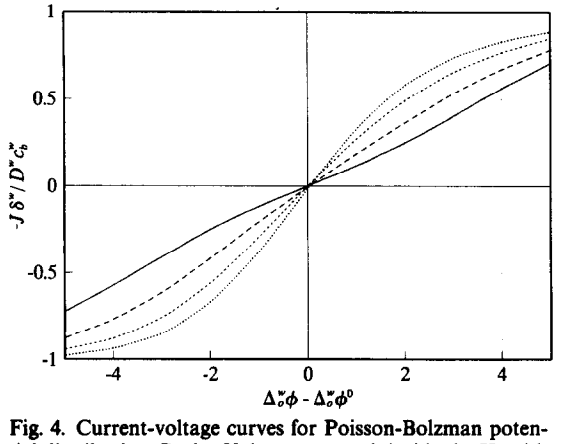

Fig. 4. Current-voltage curves for Poisson-Bolzman potential distribution, Butler-Volmer approach inside the IL with $k^0 = 10^{-2}$ cm s^{-1} and different values of α: 0.8 (solid); 0.6 (long dashed); 0.4 (dashed); 0.2 (dotted).

$$\phi = \phi_2^w + D\frac{x_2^w - x_2^o}{\varepsilon^w - \varepsilon^o} \times \ln\left[1 + \left(\frac{\varepsilon^w}{\varepsilon^o} - 1\right)\frac{x - x_2^o}{x_2^w - x_2^o}\right] \quad x_2^o < x < x_2^w \quad (14b)$$

$$\phi = 4\tanh^{-1}\{\tanh(\phi_2^o/4)\exp[\kappa^o(x - x_2^o)]\} \quad x < x_2^o \quad (14c)$$

where $\kappa^w = (2F^2c_\pm^w/\varepsilon^w\varepsilon_0 RT)^{1/2}$ and $\kappa^o = (2F^2c_\pm^o/\varepsilon^o\varepsilon_0 RT)^{1,2}$ are the inverse Debye lengths, and $c_\pm^w$ and $c_\pm^o$ the base electrolyte concentrations in the respective phase; ε_0 is the vacuum permittivity, and

$$D \equiv 2\varepsilon^o\kappa^o\sinh(\phi_2^o/2) = 2\varepsilon^w\kappa^w\sinh[(\Delta_o^w\phi - \phi_2^w)/2] \quad (15)$$

is the electric displacement in the IL. Note that the relative permittivity has been assumed to vary linearly from ε^o to ε^w across the IL. If the linear profile is also assumed for the standard transfer potential ϕ^0 as

$$\phi^0 = \begin{cases} \Delta_o^w\phi^0 & x > x_2^w \\ \Delta_o^w\phi^0\dfrac{x - x_2^o}{x_2^w - x_2^o} & x_2^o < x < x_2^w \\ 0 & x < x_2^o \end{cases} \quad (16)$$

the following expressions can be obtained after some cumbersome algebra:

$$P_{DBL}^w = \frac{D^w}{\left[x_b^w - x_2^w - \dfrac{2}{\kappa^w}(1 - e^{-(\Delta_o^w\phi - \phi_2^w)/2})\right]e^{\Delta_o^w\phi - \Delta_o^w\phi^0}} \quad (17)$$

$$P_{DBL}^o = \frac{D^o}{x_2^o - x_b^o + \dfrac{2}{\kappa^o}(e^{\phi_2^o/2} - 1)} \quad (18)$$

$$P_{IL}^{N-P} = \frac{D^{IL}e^{-\theta\Delta_o^w\phi^0}\theta^\beta(\Delta_o^w\phi^0)^{\beta+1}}{(x_2^w - x_2^o)\{\gamma[\beta + 1, (\theta + 1)\Delta_o^w\phi^0] - \gamma(\beta + 1, \theta\Delta_o^w\phi^0)\}} \quad (19)$$

where $\theta \equiv \varepsilon^o(\varepsilon^w - \varepsilon^o)$, $\beta \equiv D(x_2^w - x_2^o)/(\varepsilon^w - \varepsilon^o)$, and γ is the incomplete Gamma function.

Figure 2 shows the J vs. $\Delta_o^w\phi - \Delta_o^w\phi^0$ curves in a dimensionless form for $D^w = D^o = 10^{-5}$ cm^2 s^{-1}, and different values of D^{IL}. The following parameter values have been used: $x_b^w - x_2^w = x_2^o - x_b^o = 10^{-3}$ cm, $x_2^w - x_2^o = 1$ nm, $1/\kappa^o = 1$ nm, $1/\kappa^w = 3$ nm, and $c_\pm^w = c_\pm^o = 10$ mM. The solid line corresponds to a calculation with no inner layer and can also be interpreted as the limit of the patterned lines when D^{IL} tends to infinity. Since $P_{DBL}^w \approx P_{DBL}^o \approx 10^{-2}$ cm s^{-1} when $\Delta_o^w\phi = \Delta_o^w\phi^0$, and $P_{IL}^{N-P} \approx D^{IL}/(x_2^w - x_2^o) = 10^7$ cm^{-1} D^{IL}, Fig. 2 clearly shows that IL effects are important only if $D^{IL} < 10^{-8}$ cm^2 s^{-1}. But if the IL is taken as a mixed solvent layer flanked by aqueous and organic solutions and

$D^{o,w} \approx 10^{-5}\,cm^2\,s^{-1}$, it is hard to explain why D^{IL} should take that low values.

Analogously, the ion flux can be calculated from Butler-Volmer description making user of equations (11), (17–18). Figure 3 shows the simulation with the same parameter values as in Fig. 2, with $\alpha = 0.5$ and different values of k^0. The solid line corresponds to the reversible case, when $k^0 \to \infty$, and coincides with the solid line in Fig. 2. Again, IL are appreciable only when $k^0 < 10^{-2}\,cm\,s^{-1}$ which again is too low a value in the view of the latest results. Figure 4 shows the simulation with the same parameter values as in Fig. 2, while $k^0 = 10^{-2}\,cm\,s^{-1}$ and α is varied; taking $k^0 = 10^{-1}\,cm\,s^{-1}$ the effect of α is only vaguely noticeable.

LINEAR POTENTIAL DISTRIBUTION

It is reasonable to ask if the potential distribution has any effect on the results obtained in the previous section. Here the fluxes are calculated using equation (16) and replacing equations (14) by the following linear profile

$$\phi = \begin{cases} \Delta_o^w\phi & x > x_0^w \\ \Delta_o^w\phi\,\dfrac{x - x_0^o}{x_0^w - x_0^o} & x_0^o < x < x_0^w \\ 0 & x < x_0^o \end{cases} \qquad (20)$$

where x_0^w and x_0^o are the positions at the outer boundaries of the DDLs and are taken so that $x_0^w - x_2^w = 1/\kappa^w$ and $x_2^o - x_0^o = 1/\kappa^o$. In this case it is easy to show that

$$P_{DBL}^w = \frac{D^w}{(x_b^w - x_0^w)e^{\Delta_o^w\phi - \Delta_o^w\phi^0} + \dfrac{x_0^w - x_0^o}{\Delta_o^w\phi}\left(e^{\Delta_o^w\phi - \Delta_o^w\phi^0} - e^{\phi_2^w - \Delta_o^w\phi^0}\right)} \qquad (21)$$

$$P_{DBL}^o = \frac{D^o}{x_0^o - x_b^o + \dfrac{x_0^w - x_0^o}{\Delta_o^w\phi}\left(e^{\phi_2^w} - 1\right)} \qquad (22)$$

$$P_{IL}^{N-P} = \frac{D^{IL}\left(\dfrac{\Delta_o^w\phi}{x_0^w - x_0^o} - \dfrac{\Delta_o^w\phi^0}{x_2^w - x_2^o}\right)}{e^{\phi_2^w - \Delta_o^w\phi^0} - e^{\phi_2^0}} \qquad (23)$$

In Fig. 5 a simulation parallel to Fig. 2 is presented, but now the potential distribution is linear instead of Poisson-Bolzman distribution in Fig. 2. In Fig. 6 the same simulation is carried out replacing equation (23) by the Butler-Volmer permeability presented in equation (11). As can be seen, in both cases, the linear profile provides the better estimate for the tracer flux the greater P_{IL} is.

Finally, it is interesting to consider the limiting case where IL is absent, *ie*, the potential distribution is a single step of the height $\Delta_o^w\phi$ at the interface. Then,

$$P_{DBL}^w = \frac{D^w}{(x_b^w - x_0^w)e^{\Delta_o^w\phi - \Delta_o^w\phi^0}} \qquad (24)$$

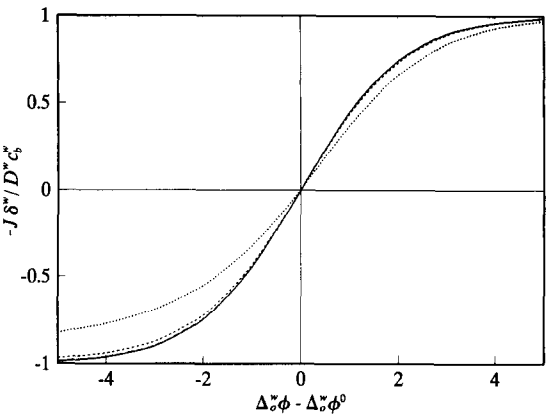

Fig. 5. As in Fig. 2, but the linear potential distribution (equation (16) and (20)).

$$P_{DBL}^o = \frac{D^o}{x_0^o - x_b^o} \qquad (25)$$

$$P_{IL}^{N-P} \to \infty \qquad (26)$$

$$P_{IL}^{B-V} = k^0 e^{(\alpha-1)(\Delta_o^w\phi - \Delta_o^w\phi^0)} \qquad (27)$$

The solid line in Fig. 5 can be viewed as representative of this stepwise profile.

APPARENT CHARGE TRANSFER COEFFICIENTS

If the flux is written using a formal kinetic equation

$$-J = k_f c_b^w - k_b c_b^o \qquad (28)$$

where k_f and k_b are the forward and backward transfer rate constants, a comparison with equation (1) gives

$$k_f = Pe^{\Delta_o^w\phi - \Delta_o^w\phi^0};\ k_b = P \qquad (29)$$

Now, comparing this with the Butler-Volmer formalism, the apparent charge transfer coefficient α_{app}

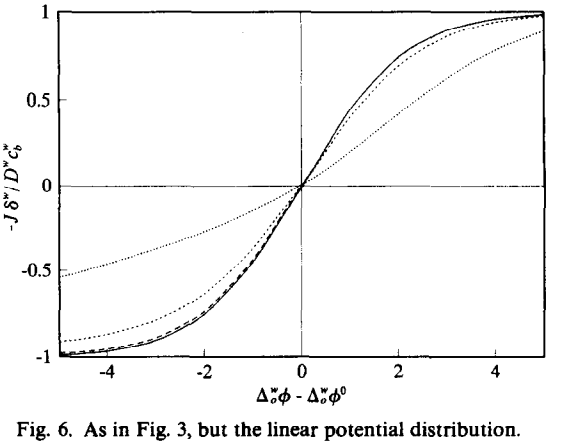

Fig. 6. As in Fig. 3, but the linear potential distribution.

is given by (see equation (12))

$$\alpha_{app} = \frac{d(\ln k_f)}{d\,\Delta_o^w\phi} = \frac{d}{d\,\Delta_o^w\phi} \times \left[\Delta_o^w\phi - \Delta_o^w\phi^0 - \ln\left(\frac{1}{P_{DBL}^w} + \frac{1}{P_{IL}} + \frac{1}{P_{DBL}^o}\right)\right] \quad (30)$$

In the case of the stepwise potential distribution this can be solved easily, and at equilibrium $\Delta_o^w\phi = \Delta_o^w\phi^0$ the results are for the Nernst-Planck approach inside the IL (see Fig. 7)

$$\alpha_{app}^{N-P} = \frac{\dfrac{x_0^o - x_b^o}{D^o}}{\dfrac{x_b^w - x_0^w}{D^w} + \dfrac{x_0^o - x_b^o}{D^o}} \quad (31)$$

and for the Butler-Volmer approach inside the IL

$$\alpha_{app}^{B-V} = \frac{\dfrac{x_0^o - x_b^o}{D^o} + \dfrac{\alpha}{k^0}}{\dfrac{x_b^w - x_0^w}{D^w} + \dfrac{x_0^o - x_b^o}{D^o} + \dfrac{1}{k^0}} \quad (32)$$

For the other cases discussed above, it is easier to simulate k_f and obtain the slope ln k_f vs. $\Delta_o^w\phi - \Delta_o^w\phi^0$ graphically. Following the trend in Fig. 7, the common feature then is the α_{app} is smaller at negative and greater at positive overpotentials than those given in equation (31) or (32), depending on the transfer mechanism through the IL.

Note that α_{app} depends on potential through the surface concentrations. In Fig. 8 the surface concentration of the tracer on the aqueous side is simulated in the case of the stepwise potential profile with $c_\pm^w = c_\pm^o$. As can be seen, the surface concentrations are very different from the bulk concentrations even assuming slow kinetic control across the IL which confirms the significance of the DBLs. When the DBLs can be eliminated, as in the case of the micro ITIES[9], the overall permeability of the system increases, resulting in high rates of transfer. Our own preliminary measurements with the rotating diffusion cell (for the description of the set-up, see Ref. [14]) have shown that extrapolating to the infinite rotating speed, where the thickness of the DBLs approaches zero, very high current densities are obtained. These measurements are still underway and will appear in a subsequent paper.

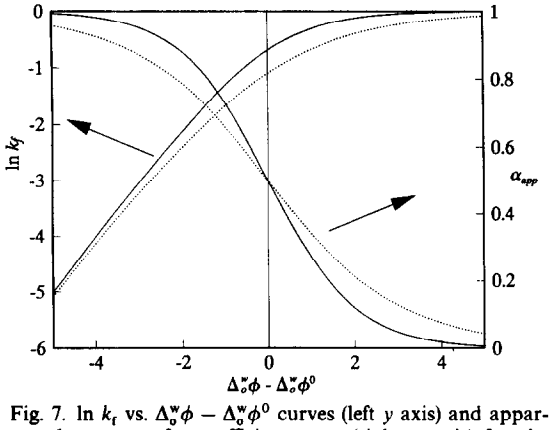

Fig. 7. ln k_f vs. $\Delta_o^w\phi - \Delta_o^w\phi^0$ curves (left y axis) and apparent charge transfer coefficients α_{app} (right y axis) for the stepwise potential distribution. Solid lines: equation (26), dotted lines: equation (27) with $k^0 = 10^{-2}$ cm s^{-1} and $\alpha = 0.5$.

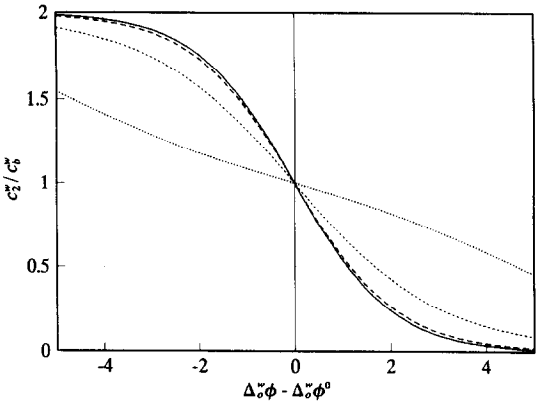

Fig. 8. Surface concentration of the tracer on the aqueous side in the case of the stepwise potential profile when $c_\pm^w = c_\pm^o$: reversible (solid), $k^0 = 10^{-1}$ (long dashed), 10^{-2} (dashed) and 10^{-3} (dotted cm s^{-1}. The concentration on the organic side is symmetrical' with respect to the zero overpotential line.

DISCUSSION

The simulations above show that the inner layer is hardly recognizable when realistic parameter values are used for the estimation of the permeabilities of the different layers. This is not surprising in the view of equation (12): first, the thickness of the IL is several orders of magnitude smaller than the thickness of the DBLs, and second, the potential drop across the IL is small, as frequently mentioned in the literature[1]. Both of these factors make the integral in equation (9) negligible when compared with the those in equation (7) and (8), and D^{IL} cannot compensate for this difference. If Butler-Volmer type equation is used for the flux across the IL, a simple order of magnitude analysis shows that k^0 should be less than *ca.* 10^{-2} cm s^{-1} to make IL 'visible'. In the simulations, we have assumed the thickness of the DBLs to be 10^{-3} cm (while they are typically of the order of 10^{-2} cm [15]) to emphasize the contribution of the IL.

In the absence of the effect of the IL the potential distribution also has very small significance because the thickness of the DDL, where the potential distribution takes place, is only a few Debye lengths, *ie* a few nanometers. In the simulations, $c_\pm^w = c_\pm^o =$ 0.01 M which is the practical lower limit for the base electrolyte in order for the trace-ion assumption to be valid (trace-ion concentration $< 2\%$ of the base electrolyte concentration) but still to have detectable currents; higher concentrations correspond to shorter Debye lengths accordingly. This means that the potential distribution can be approximated by a stepwise profile with sufficient accuracy, and that Frumkin correction is not important at steady state.

If the IL were visible, then the potential distribution would be important (compare Figs. 2 and 5 or 3 and 6) because it affects the potential drop across the IL and the assumption of the inner layer as an ion free layer in equation (13b) should be reconsidered.

Hence, the shape of the current-voltage curve resembles an apparent Butler-Volmer behaviour, but has its origin in the concentration polarization. Even if there were kinetic control of the current at the interface, or if the interfacial region imposed an extra friction to the ionic movement, the always present transport in the DBLs would screen these phenomena.

It is interesting that the apparent charge transfer coefficient α_{app} can also be obtained from the present model. This coefficient is potential dependent and has a value of *ca.* 0.5 in the vicinity of the equilibrium, as in Ref. [10], because it is determined by the potential dependent permeabilities in the different layers (see equation (30)). At the equilibrium the driving force of the transfer is zero, and the ion 'sees' only the interfacial structure in terms of the permeabilities. Equation (31) can be rewritten in the form of

$$\alpha_{app}^{N-P} = \frac{P_{DBL}^{w}}{P_{DBL}^{w} + P_{DBL}^{o}} \tag{33}$$

So, equal permeabilities in the DBLs mean a symmetrical potential barrier which has to be overcome, resulting in the value 0.5 for α_{app}. If the Butler-Volmer type equation is assumed the 'true' coefficient α is obtained at the limit $P_{DBL}^{w,o} \to \infty$ (see equation (32)).

CONCLUSIONS

It can be concluded that a steady state current-voltage curve tells very little about the interfacial structure or the mechanisms of IT unless the mass transfer resistance of the DBLs can be eliminated. Transient methods, which are not treated here, are usually utilized in order to get any information of the kinetics of IT, but these methods are, however, subject to the uncompensated *ir* drop and capacitive current which are quite difficult to take into account in the modelling of the system, as presented here. Since *ac* impedance measurements at the ITIES can be safely carried out only within the polarization window where no faradaic bias current is flowing, these are subject to only periodical concentration polarization which can be eliminated, and thus $P \equiv P_{IL}$; that is why data obtained from *ac* measurements results in higher values of k^o than those obtained from *dc* measurements[16]. The problem associated to *ac* impedance is that measurements are usually carried out in the vicinity of zero current where the structure of the interface is probably different from that in the presence of substantial flux[17]. Therefore, perhaps the most suitable methods for the study of IT in the future could be based on the use of micro ITIES[18] or a rotating diffusion cell.

Acknowledgements—Financial support from the European Union through project No. CHRX-CT92-0076, and Academy of Finland is acknowledged. Helpful discussions with Prof. D.J. Schiffrin (University of Liverpool) as well as the visit grant VAL/2501/272 from The British Council are also gratefully acknowledged.

REFERENCES

1. H. H. Girault, *Charge Transfer across Liquid/Liquid Interfaces*, in *Modern Aspects in Electrochemistry*, (Edited by J. O'M. Bockris), Vol. 25, pp. 1–62, Plenum Press, New York (1993).
2. E. J. W. Verwey and K. F. Niessen, *Philos. Mag.* **28,** 435 (1939).
3. M. Gros, S. Gromb, and C. Gavach, *J. electroanal Chem.* **89,** 29 (1978).
4. T. Kakiuchi and M. Senda, *Bull. Chem. Soc. Jpn.* **56,** 2912 (1983).
5. T. Wandlowski, V. Mareček and Z. Samec, *J. phys. Chem.* **93,** 291 (1989).
6. H. H. Girault and D. J. Schiffrin, *J. electroanal. Chem.* **150,** *43 (1983).*
7. I. Benjamin, *J. Chem. Phys.* **97,** 1432 (1992).
8. Z. Samec and V. Mareček, *J. electroanal. Chem.* **200,** 17 (1986).
9. H. H. Girault, Lecture at the 45th ISE Meeting, Porto (1994).
10. T. Kakiuchi, *J. electroanal. Chem.* **322,** 55 (1992).
11. I. Benjamin, *J. Chem. Phys.* **96,** 577 (1992).
12. P. Delahay, *Double Layer and Electrode Kinetics*, Ch. 9 Wiley-Interscience, New York, (1965), J. Koryta and P. Vanýsek, in *Advances in Electrochemistry and Electrochemical Engineering* (Edited by H. Gerischer and C. W. Tobias), Vol. 12, p. 140 Wiley- Interscience, (1988).
13. M. J. Spaarnay, *Trans. Faraday Soc.* **53,** 306 (1957); J. Newman, *ibid.* **61,** 2229 (1965); H. Matsuda and P. Delahay, *J. phys. Chem.* **64,** 332 (1960).
14. J. A. Manzanares, K. Kontturi, S. Mafé, V. M. Aguilella and J. Pellicer, *Acta Chem. Scand.* **45,** 115 (1991).
15. N. Ibl and O. Dossenbach, *Convective Mass Transport*, in *Comprehensive Treatise of Electrochemistry*, (Edited by E. Yeager), Vol. 6, pp. 133–237, Plenum Press, New York (1983).
16. T. Wandlowski, V. Mareček and Z. Samec, *J. electroanal. Chem.* **242,** 291 (1988).
17. I. Benjamin, *Chem. Phys.* **180,** 287 (1994).
18. M. C. Osborne, Y. Shao, C. M. Pereira and H. H. Girault, *J. electroanal. Chem.* **364,** 155 (1994).